Supporting Materials

S1. Effect of temperature on the impedance responses of humidity sensor.

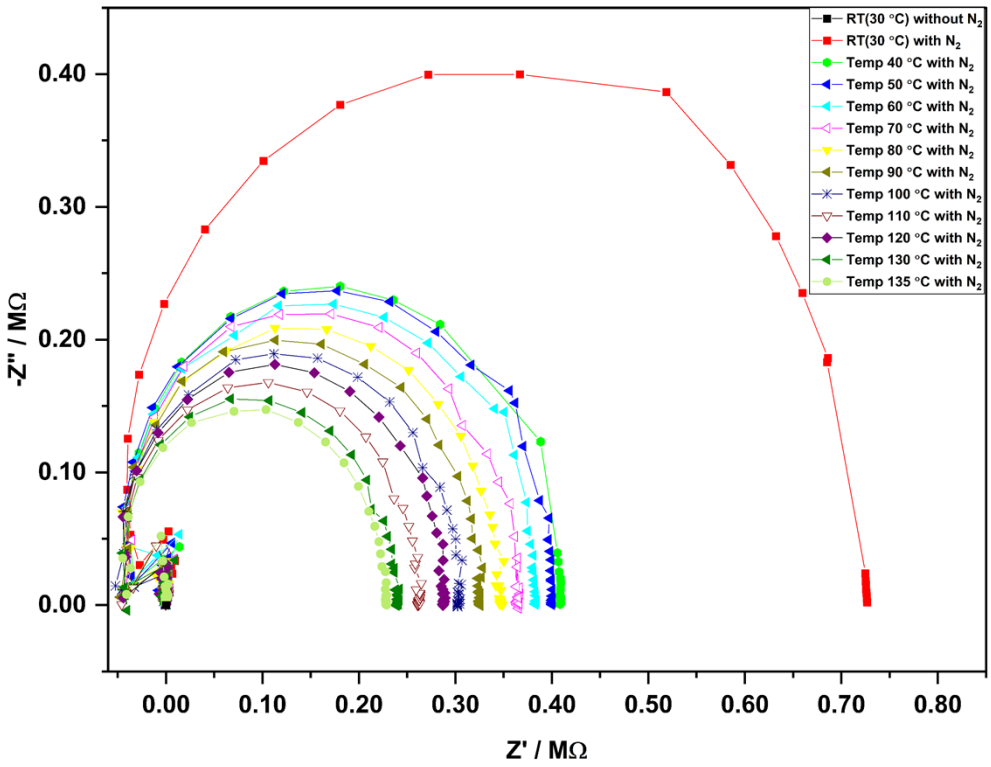

Figure S1: Impedance spectra (negative imaginary impedance vs real impedance) of the sensor at different temperatures in the presence and absence of N_2 gas.

The first impedance spectrum was collected at room temperature (30 °C) without flowing N_2 gas. It can not be clearly seen in figure S1 as it has relatively low impedance values (100 – 200 Ω) compared to other spectra that contain impedance values in MΩ level. Figure S2 shows the impedance spectrum at room temperature without N_2 gas. The other spectra were collected in the presence of N_2 gas starting from room temperature and continuing up to 135 °C.

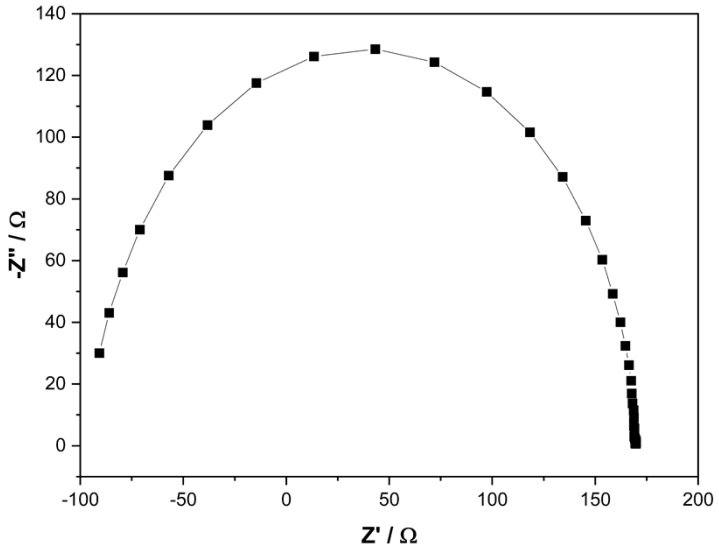

Figure S2: Impedance spectra (negative imaginary impedance vs real impedance) of the sensor at room temperature without N_2 gas.

S2. Effect of sensor substrate on sensor performance.

As a part of this study, another sensor was developed by replacing sensor substrate with transparent PET film, following the same procedures, dimensions and conditions as described in the paper-based sensor. Electrochemical impedance spectra were collected at different RH levels and analysed to identify the substrate effect. Impedance responses of this sensor were compared with the paper-based sensor to determine the effect of the sensor substrate on the sensing mechanism. With increasing humidity, the impedance of the transparent sheet-based sensor decreases. But, the impedance of the sensor is very high compared to the paper-based sensor at every humidity level. Therefore, the transparent sheet-based sensor had high resistance and low conductivity compared to the paper-based sensor even under the same humidity conditions. In accordance with these observations, it could be suggested that in the PAni film of the paper-based sensor, the mobility of the charge carriers along individual polymer chains and within adjacent chains is comparatively high. Moreover, in transparent sheet-based sensor, the linearity (R^2 values) of impedance Vs RH% plots are comparatively low indicating that impedance change with humidity is not uniform.

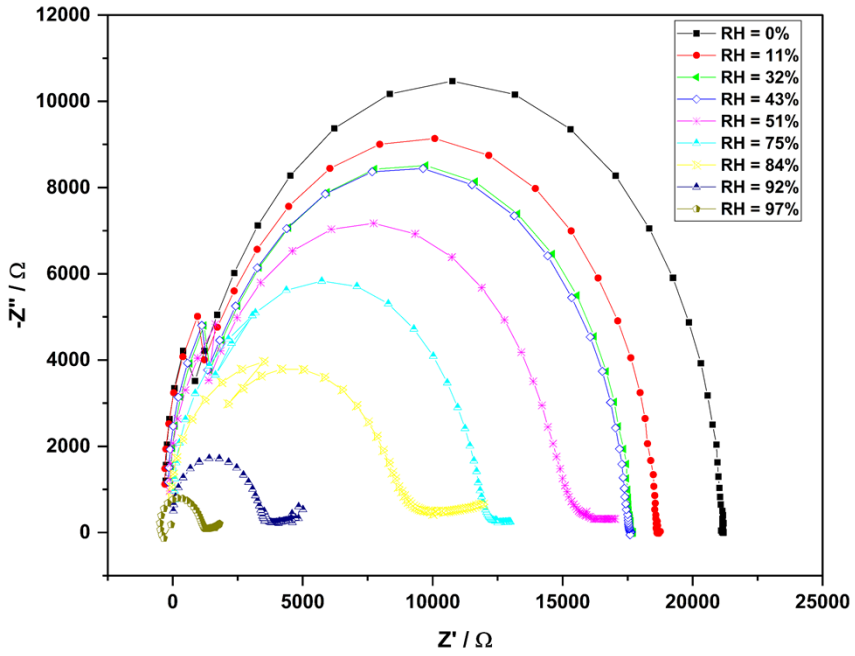

Figure S3: Impedance spectra (negative imaginary impedance vs real impedance) of the humidity sensor developed on the transparent PET sheet substrate at different humidity levels.

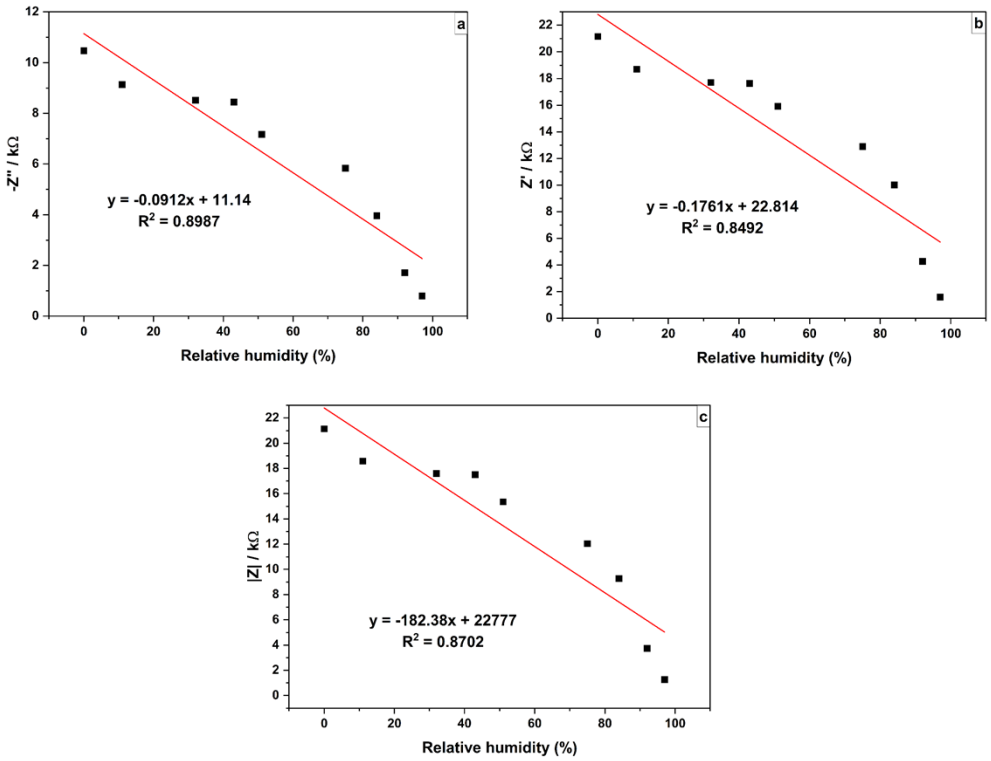

Figure S4: Variation of (a) highest -Z'' values, (b) Z' values at the intersection with the x-axis, (c) |Z| at 1000 Hz frequency of humidity sensor developed on the transparent PET sheet substrate.

S3. Hysteresis of the sensor.

Table S1: Impedance values at 1000 Hz at different humidity levels for the humidification process.

Relative humidity (%)	Impedance at 1000 Hz (Ω)
0	251.41
11	239.5
32	216.32
43	202.13
51	187.98
75	167.75
84	159.23
92	147.48
97	130.52

Table S2: Impedance values at 1000 Hz at different humidity levels for the desiccation process.

Relative humidity (%)	Impedance at 1000 Hz (Ω)
0	251.41
11	238.65
32	214.25
43	199.85
51	184.7
75	164.22
84	156.32
92	145.71
97	130.52

S4. Stability of the sensor.

Table S3: Impedance values at 1000 Hz at 11%, 75% and 97% RH levels over 30 days.

Day	Impedance at 1000 Hz (Ω)		
	RH = 11 %	RH = 75 %	RH = 97 %
1	239.5	167.75	130.52
5	239.56	166.82	131.02
10	238.28	167.71	130.52
15	238.38	166.8	129.52
20	240.38	168.45	131.41
25	240.66	163.99	128.65
30	240.74	164.74	133.27

S5. Repeatability of the sensor between 11% and 75% RH levels.

Table S4: Impedance values at 1000 Hz with time for the sensor switching between 11% and 75% RH levels.

	Time (s)	Impedance at 1000 Hz (Ω)		Time (s)	Impedance at 1000 Hz (Ω)		Time (s)	Impedance at 1000 Hz (Ω)
1	50	237.25	**26**	1300	167.74	**51**	2550	166.87
2	100	237.84	**27**	1350	204.53	**52**	2600	166.58
3	150	238.16	**28**	1400	228.13	**53**	2650	166.58
4	200	238.24	**29**	1450	235.67	**54**	2700	166.47
5	250	200.54	**30**	1500	239.26	**55**	2750	205.14
6	300	185.36	**31**	1550	240.12	**56**	2800	229.84
7	350	177.84	**32**	1600	240.15	**57**	2850	235.47
8	400	171.95	**33**	1650	208.64	**58**	2900	238.86
9	450	168.54	**34**	1700	192.54	**59**	2950	239.8
10	500	167.7	**35**	1750	180.17	**60**	3000	239.85
11	550	167.74	**36**	1800	170.45	**61**	3050	204.35
12	600	167.84	**37**	1850	167.75	**62**	3100	188.9
13	650	201.75	**38**	1900	167.51	**63**	3150	179.21
14	700	228.03	**39**	1950	167.4	**64**	3200	171.98
15	750	235.26	**40**	2000	167.39	**65**	3250	167.96
16	800	238.67	**41**	2050	210.14	**66**	3300	167.86
17	850	239.01	**42**	2100	229.01	**67**	3350	167.78
18	900	239.15	**43**	2150	234.74	**68**	3400	167.71
19	950	202.87	**44**	2200	238.35	**69**	3450	205.69
20	1000	188.2	**45**	2250	238.87	**70**	3500	229.00
21	1050	178.26	**46**	2300	238.9	**71**	3550	234.67
22	1100	172.19	**47**	2350	206.24	**72**	3600	237.54
23	1150	168.34	**48**	2400	191.07	**73**	3650	238.48
24	1200	167.42	**49**	2450	179.86	**74**	3700	238.52
25	1250	167.74	**50**	2500	171.98			

S6. Response reversibility of the sensor

Table S5: Impedance values at 1000 Hz with time for switching the sensor back and forth between RH 0% and continuously increasing RH levels for the 11-97% range.

	Time (s)	Impedance at 1000 Hz (Ω)		Time (s)	Impedance at 1000 Hz (Ω)		Time (s)	Impedance at 1000 Hz (Ω)		Time (s)	Impedance at 1000 Hz (Ω)
1	50	250.74	**30**	1500	251.45	59	2950	212.36	88	4400	178.05
2	100	251.56	**31**	1550	226.97	60	3000	186.84	89	4450	164.59
3	150	251.6	**32**	1600	213.97	61	3050	178.54	90	4500	156.9
4	200	251.64	**33**	1650	207.91	62	3100	173.21	91	4550	150.03
5	250	246.32	**34**	1700	203.26	63	3150	169.14	92	4600	148.36
6	300	242.56	**35**	1750	202.75	64	3200	168.25	93	4650	147.83
7	350	239.95	**36**	1800	202.38	65	3250	168.43	94	4700	147.75
8	400	239.64	**37**	1850	202.25	66	3300	168.26	95	4750	203.45
9	450	239.72	**38**	1900	202.23	67	3350	210.45	96	4800	226.04
10	500	239.64	**39**	1950	228.62	68	3400	240.35	97	4850	241.57
11	550	239.58	**40**	2000	246.13	69	3450	247.94	98	4900	249.14
12	600	248.47	**41**	2050	251.34	70	3500	250.26	99	4950	250.08
13	650	251.26	**42**	2100	251.25	71	3550	250.89	100	5000	250.12
14	700	251.43	**43**	2150	251.4	72	3600	250.97	101	5050	190.21
15	750	251.56	**44**	2200	251.58	73	3650	212.57	102	5100	165.37
16	800	251.66	**45**	2250	224.12	74	3700	184.51	103	5150	153.87
17	850	235.64	**46**	2300	203.47	75	3750	172.87	104	5200	145.53
18	900	225.31	**47**	2350	195.98	76	3800	165.36	105	5250	137.64
19	950	219.24	**48**	2400	189.96	77	3850	159.87	106	5300	132.54
20	1000	216.98	**49**	2450	188.36	78	3900	158.96	107	5350	131.52
21	1050	216.34	**50**	2500	188.64	79	3950	158.82	108	5400	131.47
22	1100	216.3	**51**	2550	188.12	80	4000	158.89	109	5450	185.36
23	1150	216.26	**52**	2600	188.25	81	4050	220.53	110	5500	221.98
24	1200	216.38	**53**	2650	220.46	82	4100	238.01	111	5550	238.64
25	1250	231.98	**54**	2700	244.87	83	4150	246.68	112	5600	246.29
26	1300	246.56	**55**	2750	252.02	84	4200	250.42	113	5650	249.1
27	1350	251.28	**56**	2800	252.16	85	4250	251.16	114	5700	249.73
28	1400	251.36	57	2850	251.84	86	4300	251.23			
29	1450	251.14	58	2900	252.21	87	4350	200.54			

S7. SEM analysis of the PAni film.

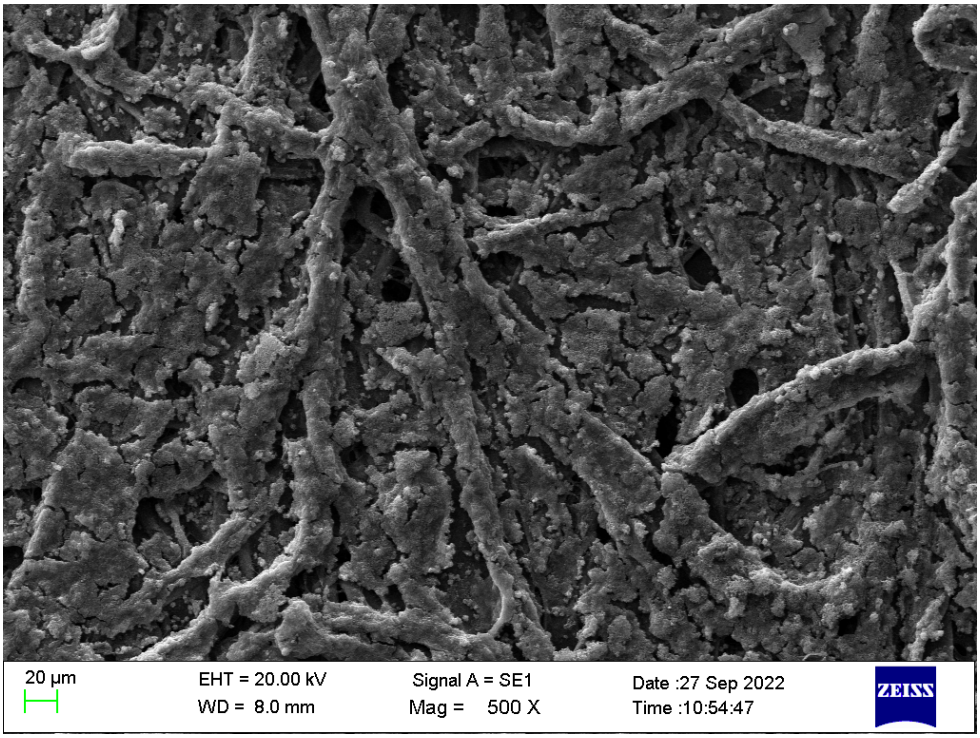

Figure S5: SEM images of the PAni film with low magnification (500 X).

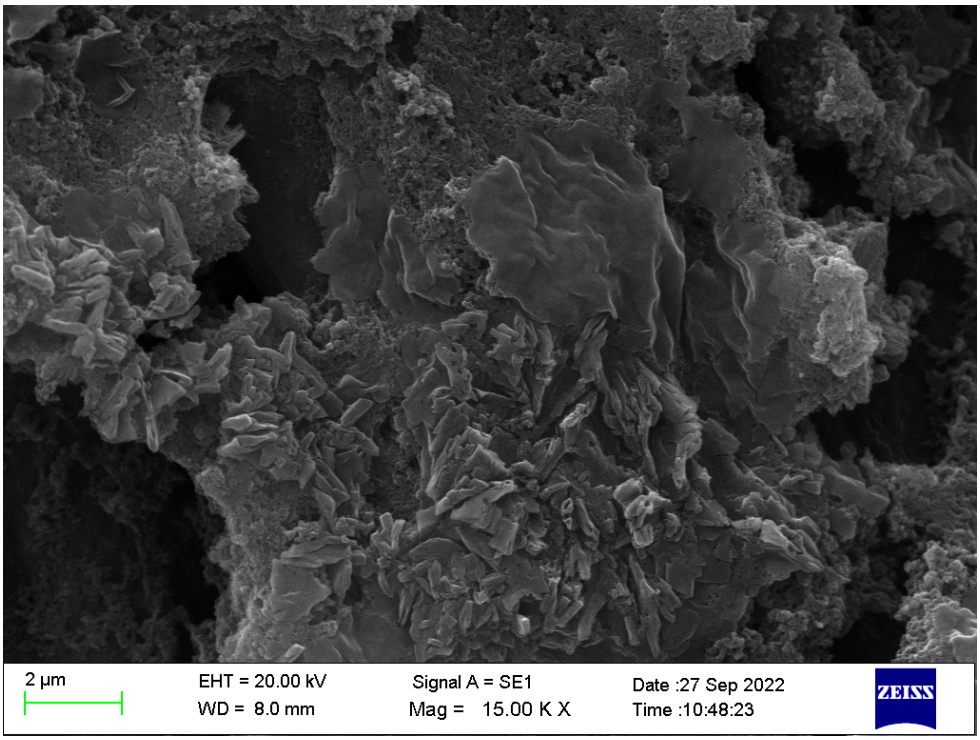

Figure S6: SEM images of the PAni film with high magnification (15.00 KX).

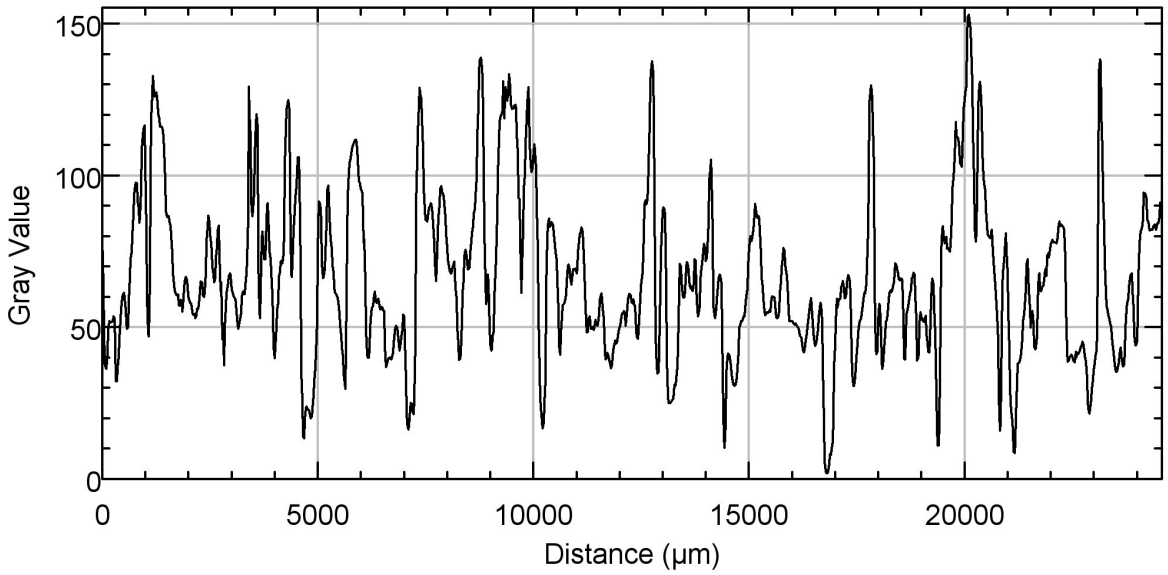

Figure S7: Surface roughness profile.

Figure S7 shows the surface roughness profile generated along with ImageJ software (Roughness calculation plugin).

S8. Response percentage/ Responsivity calculation.

The response percentage of the sensor was calculated as follows.

%Response = $((R_i - R_f)/R_i)$ X 100

Here, R_i and R_f are the resistance/impedance of the sensor under initial/dry state and moist state, respectively.